Environmental Science & Technology

Article

pubs.acs.org/est

Phototransformation Rates and Mechanisms for Synthetic Hormone Growth Promoters Used in Animal Agriculture

Shen Qu,[†] Edward P. Kolodziej,[‡] and David M. Cwiertny*[,†]

[†]Department of Civil and Environmental Engineering, University of Iowa, 4105 Seamans Center, Iowa City, Iowa 52242, United States

[‡]Department of Civil and Environmental Engineering, University of Nevada, Reno, Reno, Nevada 89557, United States

Supporting Information

ABSTRACT: Trenbolone acetate, melengestrol acetate, and zeranol are synthetic hormones extensively used as growth promoters in animal agriculture, yet despite occurrence in water and soil little is known about their environmental fate. Here, we establish the time scales and mechanisms by which these synthetic growth promoters and their metabolites (SGPMs) undergo phototransformation in sunlit surface waters. The families of trenbolone acetate (including 17β-trenbolone, 17α-trenbolone, and trendione) and melengestrol acetate (including melengestrol) readily undergo direct photolysis, exhibiting half-lives between ~0.25 and 1 h in both natural and simulated sunlight that were largely insensitive to solution variables (e.g., pH, temperature, and cosolutes). Direct photolysis yielded products that not only are more photostable but also maintain their steroidal ring structure and therefore may retain some biological activity. In contrast, zeranol, β-zearalanol, and zearalanone only exhibited reactivity in irradiated solutions of model humic and fulvic acids, and rates of indirect photolysis increased steadily from pH 7 to 9. Use of selective probe and quencher compounds suggest hydroxyl radical and triplet state dissolved organic matter are responsible for zeranol family decay at neutral pH, although singlet oxygen contributes modestly in more alkaline waters. This observed pH-dependence appears to result from photooxidants reacting primarily with the monodeprotonated form of zeranol (pK_a values of 8.44 and 11.42). This investigation provides the first characterization of the fate of this emerging pollutant class in sunlit surface waters and prioritizes future efforts on the identity, fate, and biological impact of their more persistent phototransformation products.

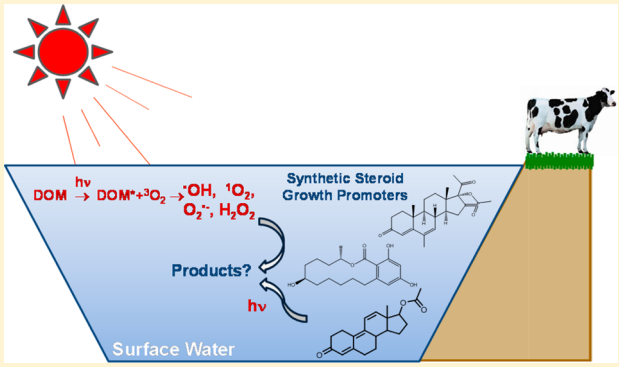

INTRODUCTION

Growth promoters are used extensively in animal agriculture to improve feed efficiency, weight gain, and muscle-to-fat ratio.[1−4] They include natural and synthetic hormones, and it is estimated that over 97% of U.S. beef cattle receive such supplements.[5] A particularly potent subset of growth promoters are the anabolic synthetic hormones, of which the U.S. Food and Drug Administration has approved three for use in cattle and sheep raised for meat production.[6] These are trenbolone acetate (TBA), an androgenic steroid with anabolic potency 8-to-10-fold greater than testosterone propionate,[7] the progestin melengestrol acetate (MGA) with activity in cattle 125-fold greater than progesterone,[8] and zeranol, a nonsteroidal, resorcyl lactone derived from the mycotoxin zearalenone, which functions as an estrogen (Table 1).

After application, some of these growth promoters can be excreted unmetabolized, although most mass is excreted as various metabolites. In studies with heifers using radiolabeled TBA, 80% of the intravenously administered dose (based on radioactivity) was excreted in bile within 24 h, but all was metabolized; 17α-trenbolone (33% of excreted radioactivity) was the dominant metabolite, while 17β-trenbolone (0.9%), which represents the biologically active form of TBA, and trendione (1.2%) appeared in smaller quantities.[9] For MGA, about 10−17% of the administered dose was excreted in feces unmetabolized,[10] where once in the environment it may hydrolyze at slightly basic pH (~8 or 9) to melengestrol.[11] Zeranol (25 mg/d) dosed to heifers yielded 2−5 μg/L of unmetabolized zeranol in urine, with β-zearalanol (2−5 μg/L) and zearalanone (0.1−0.5 μg/L) metabolites also observed.[12]

Because of their widespread application, their high administered dose (e.g., 36−72 mg/implant, 140−200 mg/implant, and 0.5 mg/day for zeranol, trenbolone acetate, and melengestrol acetate, respectively)[2,13] and the large number of cattle receiving implants annually, the discharge of synthetic growth promoters and their metabolites (hereafter SGPMs) into the environment is a certainty. Indeed, there are a growing number of reports of their occurrence in surface waters and soil near animal agriculture operations on the order of 10−100 ng/

Received: July 30, 2012
Revised: November 15, 2012
Accepted: November 19, 2012

   dx.doi.org/10.1021/es303091c | Environ. Sci. Technol. XXXX, XXX, XXX−XXX

Table 1. Structures of Synthetic Growth Promoters and Their Metabolites (SGPMs) Considered Herein

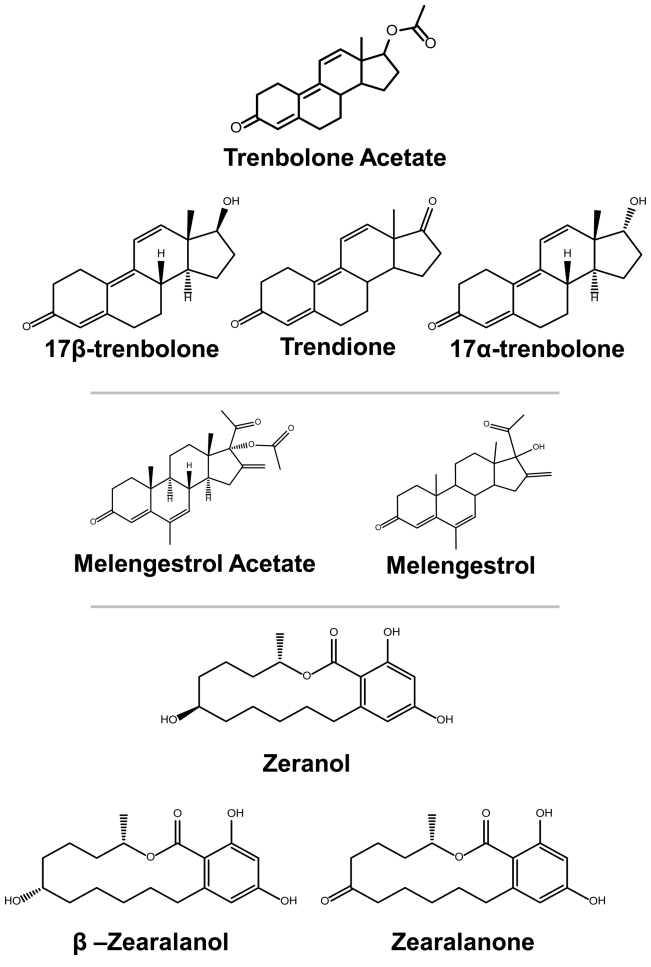

L and 1−100 ng/kg level, respectively,[14−19] raising concerns over potential ecosystem health risks because of their anabolic potency.[6,15,17,20−23] For example, Ankley et al. reported that 17α- and 17β-trenbolone are reproductive toxicants in fish that result in decreased fecundity in the female fathead minnow at 10−30 ng/L concentrations.[20,22]

Given the limited information available on their persistence in surface waters, assessing the ecosystem impacts of this emerging pollutant class remains challenging. Photolysis likely represents a major attenuation pathway for SGPMs, yet little information exists about the rates, mechanisms, and products of photolysis as well as how solution variables (e.g., pH and cosolutes) influence these processes. Outside of limited data for the photolysis of 17β-trenbolone and zeranol in cattle urine[24] and the decay of 17β-trenbolone with 254 nm light during simulated UV treatment,[25] most information on SGPM photolysis comes from the manufacturer's environmental assessment report produced at the time of the chemical's market introduction.[11,26,27] These reports indicate the possibility of direct photoreaction for TBA and MGA, but fundamental details about these photoreactions were not rigorously explored. For example, these reports only considered direct photolysis (i.e., absorption of light to break or rearrange bonds within the chemical structure) and ignored the potential importance of indirect photolysis pathways (i.e., light is first absorbed by another chromophore that then initiates reaction via energy transfer to another species). Furthermore, these reports rarely considered metabolite photoactivity, and these may be the species most likely encountered in surface waters.

The overall objective of this study is to establish the time scales and dominant mechanism of photolysis for the suite of nine SGPMs in Table 1. In batch photoreactors using both natural and simulated sunlight, we identify those species prone to direct photolysis and quantify their half-lives ($t_{1/2}$ values) and quantum yields (Φ values) for this process. Indirect photolysis was probed using a suite of model humic and fulvic acids as sources of possible reactive entities including reactive oxygen species (ROS) and triplet state DOM (^{3}DOM*). The specific species responsible for indirect photolysis were then assessed using standard probe compounds to quantify steady-state concentrations of transient ROS in our photoreactors as well as through the use of selective quenchers to suppress the activity of specific photooxidants toward SGPMs. We explore the effects of common environmental variables (e.g., temperature, pH, cosolutes) on these processes and compare the rates and pathways observed in model laboratory systems to results obtained using two natural water samples with varying levels of dissolved organic carbon (DOC). Finally, we provide an initial description of transformation products generated via direct photolysis, but a more detailed treatment of these transformation products will be provided in a future study.

EXPERIMENTAL PROCEDURES

Reagents. A complete list of reagents is provided in the Supporting Information. All SGPMs were acquired from commercial sources, of high purity, and used as received. We note that because TBA is not typically excreted unmetabolized,[9] it was included in only a select number of experiments to compare its behavior to that of its major metabolites.

Direct Photolysis Experiments. Rates and products of direct photolysis were explored using both simulated and natural sunlight. The majority of experiments were conducted using a commercially available 450 W xenon arc lamp (Newport Corporation). The light was first passed through a water filter to remove IR radiation, reflected off a 90° full reflectance beam turning mirror, and then passed through an AM 1.5 filter and a 305 nm long-pass filter to generate a spectrum of light more closely resembling that available at the earth's surface. Photon rates were measured by chemical actinometry using ferrioxalate,[28] yielding a photon flux of 3.9×10^{-4} photons/m^2 s (6.5×10^{-28} einsteins/m^2 s) when normalized to the incident area of the photoreactor.

Unless noted, all photochemical experiments were conducted in a water-jacketed, borosilicate photoreactor (37 mm inner diameter × 67 mm depth for a nominal volume of ∼50 mL; Chemglass), whose contents were mixed via a magnetic stirrer and stir plate during all experiments. Experiments used 20 mL of SGPM solutions in 5 mM phosphate buffer (prepared as described in the Supporting Information), with the majority conducted at pH 7.0 and 25 °C. The system temperature was held constant via a recirculating water bath. Upon irradiation, aliquots of solution (∼1 mL) were withdrawn at periodic intervals and transferred to a 2.5 mL amber autosampler vial for subsequent analysis via HPLC with a photodiode array detector (HPLC-DAD) or LC with detection via tandem mass spectrometry (LC/MS/MS). Typical initial concentrations in photolysis experiments were 1−10 μM (on the order of ∼0.3−30 mg/L). Although these concentrations are greater than those previously reported in surface waters, they were necessary to facilitate HPLC-DAD analysis, which was the method best

dx.doi.org/10.1021/es303091c | Environ. Sci. Technol. XXXX, XXX, XXX−XXX

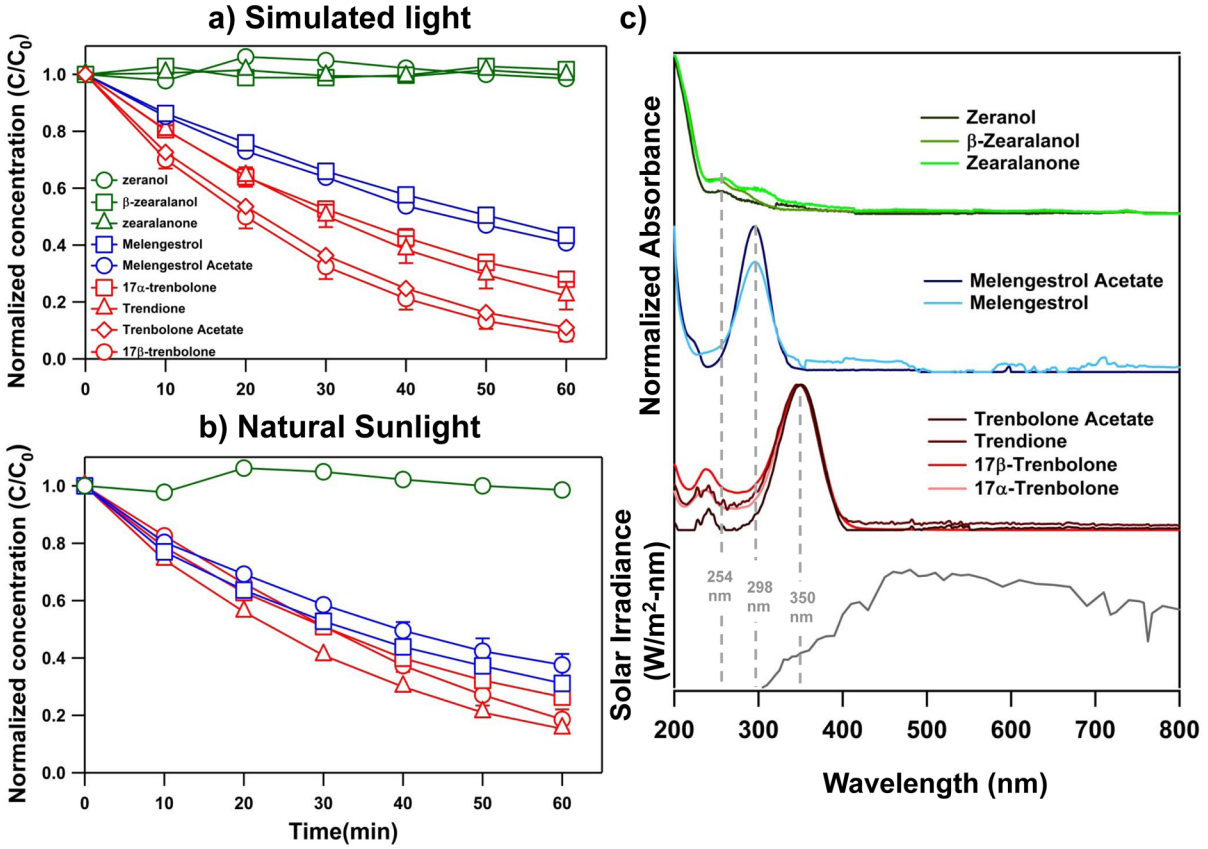

Figure 1. Concentration profiles of SGPMs as a function of irradiation by (a) simulated sunlight and (b) natural sunlight in 5 mM phosphate buffer at pH 7. Only a subset of SGPMs was considered in natural sunlight to verify trends and time scales observed with the simulated light source. (c) UV−visible light absorption spectra collected for all SGPMs in Milli-Q water. Noted in panel c are the primary absorbance maxima for each compound class, and the solar irradiance available at the earth's surface is provided for comparison (ASTM reference spectra G173-03). Uncertainties represent 1 standard deviation of at least duplicate experiments. If uncertainties are not visible, they are smaller than the symbol. Additional experimental conditions are provided in the text and the Supporting Information.

suited for processing the large number of samples generated in our kinetic studies. We note that a possible risk of working at these relatively high concentrations is that self-quenching or self-screening could affect the degradation rates and quantum yields reported herein. However, a limited number of experiments conducted at environmentally relevant conditions (~nanomolar levels) for a subsequent study yielded comparable reactivity to that observed in this study. Thus, we do not believe these phenomena to be significant in our more concentrated systems. When possible experiments were conducted in triplicate, but limitations in the amount of certain chemicals arising from their cost sometimes resulted in fewer replicates. Control experiments were conducted with each SGPM in the dark (i.e., not irradiated) systems.

For species observed to undergo direct photolysis, additional experiments with simulated sunlight explored the effect of common environmental variables on this process. The variables included temperature (10 °C), pH (5, 7, 9), and the presence of cosolutes. Cosolutes were considered across environmentally relevant concentrations and included bicarbonate (HCO_3^-, up to 30 mg/L HCO_3^-), nitrate (NO_3^-, up to 50 mg/L NO_3^-), phosphate [up to 125 μg/L as P using a DI water background (i.e., without phosphate buffer)], and dissolved organic matter (up to 50 mg/L of Elliott soil humic acid, Leonardite humic acid, and Fluka humic acid). These model humic acids were chosen because, as will be noted subsequently, they were among the most reactive with respect to rates of indirect photolysis and also exhibited comparable absorbance (at a fixed concentration) relative to alternative forms of model organic matter. Thus, they seemed well-suited to evaluate the potential for DOM to either enhance SGPM transformation via indirect photolysis pathways or inhibit direct photolysis via light screening in our systems.

A subset of experiments examined direct photolysis via natural sunlight. Experiments were conducted in duplicate using solutions irradiated by incident sunlight over the months of June to September in Riverside, California (latitude, 34° N; longitude, 117° W; temperature = 28 ± 3 °C). Reactors were constructed and sampled as described previously for simulated sunlight, although experiments with sunlight were only conducted at pH 7.0 and a water bath rather than recirculating system was used to maintain a near constant temperature. For these experiments, the quantum yield (Φ values) was measured via the method of Leifer[29] using the binary actinometer PNA/pyridine of Dulin and Mill[30] as detailed in the Supporting Information.

Indirect Photolysis Experiments. For indirect photolysis, experiments were conducted with irradiated solutions of model dissolved organic matter (DOM). Experiments used simulated sunlight in an identical reactor to that described for direct photolysis studies. Humic acids (HA) and fulvic acids (FA) obtained from commercial sources included Fluka humic acid (FHA), Elliott soil humic acid (ESHA), Leonardite humic acid (LHA), Suwanee River humic acid (SRHA), and Suwanee

dx.doi.org/10.1021/es303091c | Environ. Sci. Technol. XXXX, XXX, XXX−XXX

Table 2. Half-Lives ($t_{1/2}$ Values) and Quantum Yields (Φ) for SGPMs Found to Undergo Direct Photolysis at pH 7.0[a]

SGPM	$t_{1/2}$ values (min)[b]		direct photolysis rate constant (min^{-1})		quantum yield (Φ)[c] $\times 10^3$
	simulated sunlight	natural sunlight	simulated sunlight	natural sunlight	
			Direct Photolysis		
trenbolone acetate	18.7 ± 1.2	NM[d]	0.037 ± 0.002	NM[d]	NM[d]
17β-trenbolone	16.9 ± 1.0	24.7 ± 3.2	0.041 ± 0.003	0.0280 ± 0.004	1.58 ± 0.16
17α-trenbolone	32.5 ± 0.8	31.1 ± 0.8	0.213 ± 0.0005	0.0223 ± 0.0006	1.49 ± 0.11
trendione	27.3 ± 1.6	22.1 ± 0.8	0.0254 ± 0.0015	0.0314 ± 0.0012	3.1 ± 0.4
melengestrol acetate	46.3 ± 1.5	42.7 ± 3.3	0.0150 ± 0.0005	0.0162 ± 0.0013	4.9 ± 0.5
melengestrol	50.4 ± 1.0	36.4 ± 2.8	0.0137 ± 0.0003	0.0190 ± 0.0015	7.8 ± 0.5
			Indirect Photolysis		
				$t_{1/2}$ values in 5 mg/L ESHA (h)[e]	
zeranol				3.24 ± 0.14	
β-zearalanol				4.1 ± 0.8	
zearalanone				4.8 ± 0.2	

[a]Also provided are $t_{1/2}$ values measured for zeranol and its metabolites in irradiated solutions of Elliot Soil Humic Acid (ESHA) at pH 7.0. [b]Photon rates measured via chemical actinometry with ferrioxalate were 4×10^{-7} photons/s for simulated sunlight generated with a Xe arc lamp and ranged between 2 and 5×10^{-7} photons/s over the course of experiments with natural sunlight (conducted between June and September in Riverside, CA). Uncertainties represent 1 standard deviation from at least duplicate experiments. [c]Reported only for natural sunlight. Uncertainties represent 95% confidence intervals from regression analysis shown in Figure S3 in the Supporting Information. [d]Not measured because trenbolone acetate is not excreted in an unmetabolized form. [e]Uncertainties represent 95% confidence intervals from regression analysis of semilog plots of concentration versus time for data shown in Figure S7 in the Supporting Information.

River fulvic acid (SRFA). Stock solutions (~200 mg/L) were prepared by dissolving known masses of each HA and FA into deionized water adjusted to pH 12 using 5 M NaOH. The mixture was then adjusted to pH 7 using 5 M HCl and subsequently diluted to produce the concentration utilized in photolysis experiments (1−10 mg/L).

Complementary experiments with each HA and FA were conducted in the absence of SGPMs to quantify the steady-state concentration of select ROS generated upon irradiation using probe compounds [e.g., phenol for hydroxyl radical ($^{\bullet}OH$) and furfuryl alcohol for singlet oxygen ($^1O_2$)]. Details on these methods are provided in the Supporting Information. The role of each ROS in SGPM transformation was assessed using selective quenchers including either formate or isopropanol (50−100 mM) for $^{\bullet}OH$, sodium azide (10 mM) for $^1O_2$, superoxide dismutase (2 U/mL) for superoxide, and catalase (200 U/mL) for H_2O_2. Isoprene (0.1% v/v) was also used to assess involvement of triplet state DOM ($^3DOM^*$). A subset of experiments was conducted in D_2O to probe further the role of $^1O_2$, whereas some were also conducted in deoxygenated systems to examine reaction pathways not involving ROS. Experiments with zeranol were also conducted as a function of pH, using 5 mM phosphate buffer at pH 7.0 and 7.5, while higher pH values (8.0−9.0) used a 5 mM borate buffer. Finally, for select SGPMs, we explored the second-order rate coefficients for reaction with $^1O_2$ and $^{\bullet}OH$ as quantified via the procedures in the Supporting Information.

Experiments in Natural Water Samples. Water samples from a runoff-impacted creek and agricultural return water collected in an irrigation canal in the Yuba River watershed (Browns Valley, CA) were also used in photolysis experiments. Immediately after collection, samples were passed through a 0.2 μm PTFE filter under vacuum. The pH values of these water samples were between pH 6.8 and 7.0, and by TOC analysis the dissolved organic carbon (DOC) contents for the creek and agricultural return water were 50 mg/L and 6 mg/L, respectively. Other characteristics of these surface waters were not measured (e.g., alkalinity and nitrate), but we expect such constituents to be present at relatively low levels because the samples were collected in winter and thus likely diluted by the seasonal rain. Photolysis experiments with these waters were conducted according to the aforementioned procedures, and dark control experiments were conducted to evaluate the possibility of alternative loss processes.

Analytical Methods. Samples were analyzed on a 1200 series Agilent HPLC-DAD equipped with an Eclipse XBD-C18 column (4.6 mm × 150 mm, 5 μm particle size) using methods for SGPMs adapted from previous studies.[31−34] Photoproducts were examined via high-resolution LC−MS/MS analysis conducted with a paradigm multi-dimensional liquid chromatography (MDLC) instrument (Michrom Bioresources, Auburn, CA) equipped with a Genesis Lightning C-18 4 μm particle 200 Å pore size (2.1 mm × 100 mm) column (Grace Davison). Eluted compounds were analyzed using an LTQ-Orbitrap XL (ThermoElectron, Bremen Germany) detector equipped with an Ion Max source (ThermoElectron) using Xcalibur v 2.0.7 software for data processing. Additional details on these analytical methods as well as those associated with measurement of ROS generated in photoreactors can be found in the Supporting Information.

RESULTS AND DISCUSSION

Direct Photolysis of SGPMs with Simulated and Natural Sunlight. Concentration profiles for SGPMs as a function of irradiation time with natural and simulated sunlight are shown in Figure 1. All SGPMs except the zeranol family were prone to direct photolysis at pH 7. For the TBA and MGA families, the loss followed exponential decay, allowing first-order rate coefficients and corresponding $t_{1/2}$ values (Table 2) for direct photolysis to be quantified from semilog plots of concentration versus time. Direct photolysis was rapid for the TBA and MGA families, producing $t_{1/2}$ values between ~0.25 and 1 h in simulated light (Figure 1a and Table 2). The TBA family was slightly, but consistently, more reactive than melengestrol acetate and melengestrol, which exhibited nearly identical photolysis rates. Within the TBA family, 17β-

dx.doi.org/10.1021/es303091c | Environ. Sci. Technol. XXXX, XXX, XXX−XXX

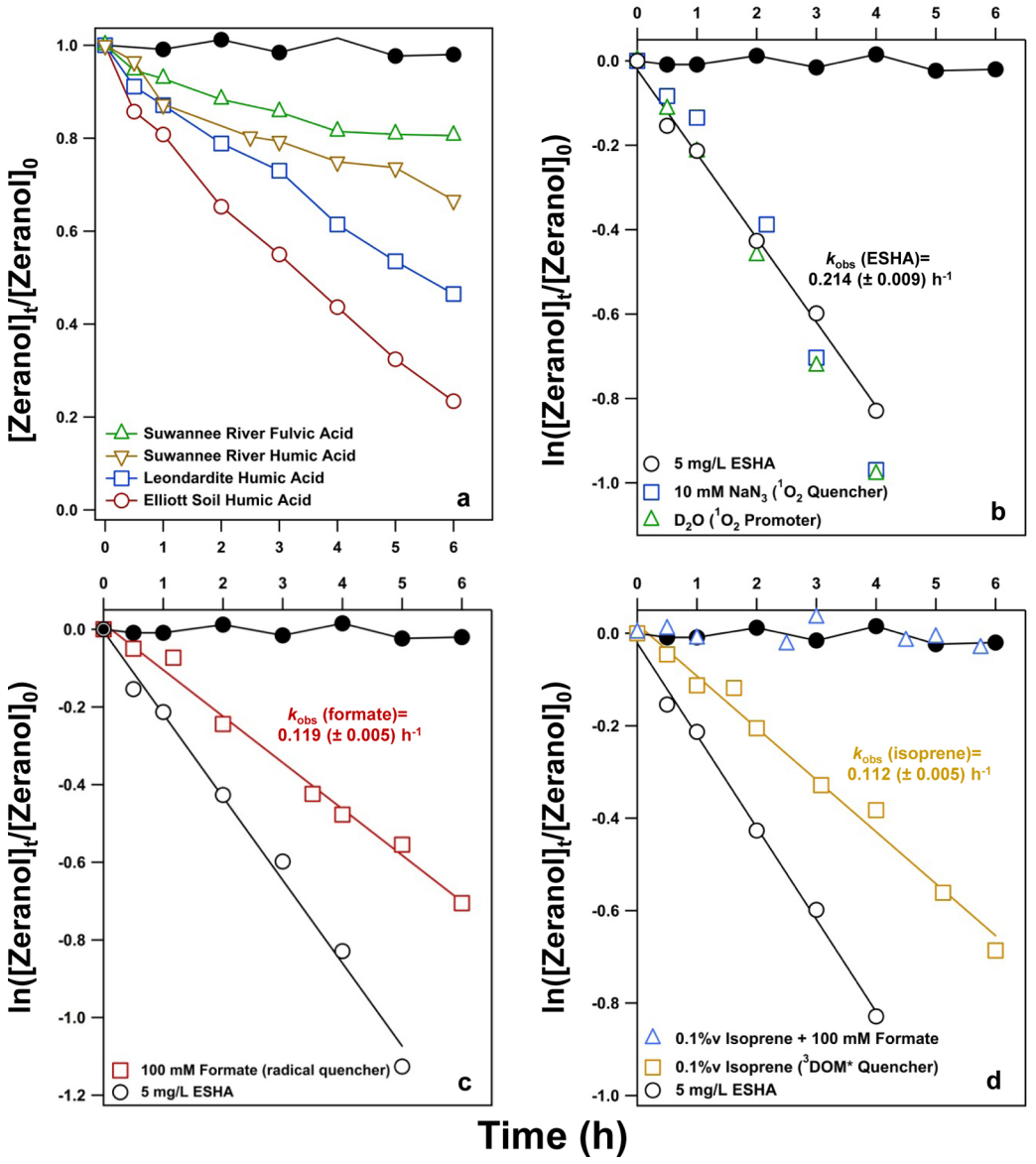

Figure 2. (a) Zeranol transformation in the presence of model humic acids (HA) and fulvic acids (FA) during irradiation with simulated light. Also shown are results of selective quencher experiments illustrating the effect of (b) 10 mM sodium azide (a singlet oxygen quencher) and D_2O (a singlet oxygen promoter), (c) 100 mM sodium formate (a hydroxyl radical quencher), and (d) 0.1% v/v of isoprene (a triplet state quencher) on zeranol transformation in the presence of ESHA irradiated with simulated light. Also in panel d, isoprene and formate, when added simultaneously, were able to entirely inhibit zeranol loss. In all instances, the initial concentration of zeranol was ~5 μM, the concentration of each HA or FA was 5 mg/L, and the pH was maintained at pH 7 using 5 mM phosphate buffer. In panels b–d, lines represent best-fit linear regressions from which pseudofirst order rate constants for zeranol decay (k_{obs} values) were obtained. Uncertainties on k_{obs} values represent 1 standard deviation of the slopes obtained from linear regression analysis. Black symbols represent controls, in which zeranol was stable in both irradiated systems without model HA and FA (i.e., direct photolysis) and in dark (i.e., nonirradiated) solutions of model HA and FA.

trenbolone and TBA photolyzed at nearly equivalent rates, which were slightly albeit significantly faster than those observed for trendione and 17α-trenbolone. SGPM decay in natural sunlight (Figure 1b) closely mirrored behavior observed with simulated light. Although TBA metabolites still exhibited greater reactivity than melengestrol acetate and melengestrol in sunlight, the reactivity difference was not as pronounced as with simulated light, presumably from minor differences in the irradiance spectra of the two light sources (see Figure S1 in the Supporting Information). Notably in all dark controls, SGPM concentrations were stable, confirming that no other transformation pathways occurred over these time scales.

These observed trends in direct photolysis can be rationalized by the relative light absorbance and photochemical quantum yields for each family of SGPMs. In Figure 1c, UV/vis absorbance spectra for each SGPM are compared to the solar irradiance available at the earth's surface, in which overlap between SGPM absorbance and available light energy is necessary for direct photoreaction. Within a family of compounds, absorbance spectra are nearly identical. All TBA family members exhibit absorbance maxima in the UV-A region at approximately 350 nm, characteristic of their conjugated 4,9,11 triene π-bond system, with secondary maxima near 240 nm. The MGA family exhibited a single absorbance maximum at 298 nm, a shift toward lower wavelengths relative to TBA

dx.doi.org/10.1021/es303091c | Environ. Sci. Technol. XXXX, XXX, XXX–XXX

and its metabolites because of their lower degree of π-bond conjugation. This in turn produces a lesser degree of overlap with the solar spectrum than compared to the TBA family. This result is most easily seen via plots of the spectral overlap integral for each species (Figure S2 in the Supporting Information), which represents the product of the compound's molar absorptivity (ε_λ) and the light intensity (L_λ), both as a function of wavelength. In contrast, zeranol and its metabolites possess primary absorbance maxima near 254 nm, characteristic of their aromatic moiety, although a small amount of absorbance is measurable above 300 nm. Such limited absorption of the zeranol family within the solar spectrum contributes to their stability upon irradiation.

Quantum yields measured in natural sunlight (Table 2 and Figure S3 in the Supporting Information) were slightly greater for melengestrol acetate ($\sim 5 \times 10^{-3}$) and melengestrol ($\sim 8 \times 10^{-3}$) than for the trenbolone metabolites (ranging from 1.5 to 3×10^{-3}). We have assumed that these quantum yields are independent of wavelength, and we are unable to report a quantum yield for zeranol family compounds due to their lack of direct photoreactivity, even over longer irradiation time scales ($\geq$6 h). For 17β-trenbolone, the quantum yield measured herein is similar to that reported by Gryglik et al.,[25] who reported a quantum yield for 17β-trenbolone of 2.9 ($\pm$0.2) $\times 10^{-3}$ at 254 nm. The greater quantum yields for melengestrol acetate and melengestrol help to explain their minimal difference in photoactivity relative to TBA metabolites, which absorb light over a greater portion of the available solar spectrum.

These Φ values are also comparable to those reported for other natural and synthetic steroids. For example, in work with the natural androgen testosterone, Vulliet et al.[35] reported a quantum yield of 2.4×10^{-3} at 313 nm. Another reasonable comparison is to estrone, a metabolite of 17β-estradiol also prone to direct photolysis. Working with a solar simulator, Lin and Reinhard[36] measured a quantum yield for estrone of 2.96×10^{-2}, roughly twice the largest Φ value measured herein for melengestrol. Therefore, it appears the TBA and MGA families exhibit photoefficiencies that are at best equivalent to other classes of steroid hormones. However, because of their greater extent of overlap with the solar spectrum, they tend to exhibit half-lives (<1 h) that are considerably shorter than previously observed for the direct photolysis of most natural and synthetic estrogens (between 5 and 40 h in DI water)[36] and testosterone ($\sim$5 h with irradiation 313 nm light).[35]

Additional experiments were conducted with 17β-trenbolone and MGA to examine the influence of solution composition on direct photolysis rates. Essentially, rates of 17β-trenbolone transformation were invariant across a broad range of temperature (10−25 °C), pH (5, 7, 9), and cosolute concentrations including HCO_3^- (up to 30 mg/L as HCO_3^-), NO_3^- (up to 20 mg/L as NO_3^-), and phosphate (up to 125 μg/L as P) (Figure S4 in the Supporting Information). Notably, the presence of model organic matter (ESHA, LHA, and FHA ranging from 0 to 50 mg/L) exhibited neither a positive (e.g., production of photochemically reactive species) nor a substantially negative (e.g., light screening to inhibit direct photolysis) impact over the range of concentrations considered. For 17β-trenbolone, rates of photolysis were essentially invariant up to 10 mg/L of ESHA or LHA, and even 50 mg/L of FHA only inhibited the rate of photolysis by $\sim$30% (Figure S4f in the Supporting Information). MGA was slightly more prone to inhibition, exhibiting a comparable $\sim$35% decrease in direct photolysis rate at 10 mg/L of ESHA (Figure S5 in the Supporting Information). As detailed in the Supporting Information, these rate decreases appear primarily attributable to light screening, as estimated screening factors agree well with the decrease in k_{obs} values observed in organic matter containing systems. Accordingly, the greater inhibition of MGA photolysis is thereby attributable to the larger degree of humic and fulvic acid absorbance (Figure S6 in the Supporting Information) at its maximum absorbance wavelength ($\sim$300 nm) relative to that for 17β-trenbolone ($\sim$350 nm). Nevertheless, on the basis of measured half-lives in both natural and simulated light (Table 2) and the negligible to minor influence exerted by most common aquatic variables (Figures S4 and S5 in the Supporting Information), direct photolysis appears to be the dominant loss process in most sunlit surface waters for the TBA and MGA families.

Indirect Photolysis of Zeranol and its Metabolites at Neutral pH. Although they did not undergo direct photolysis, zeranol and its metabolites were reactive in irradiated solutions of humic and fulvic acids. At pH 7.0, zeranol loss was observed in all solutions (5 mg/L) of model DOM (Figure 2a), with the greatest rate of decay being observed for ESHA ($t_{1/2} \sim 3$ h) while SRFA was least active ($t_{1/2} \sim 19$ h). Comparable reactivity was also observed for β-zeralanol and zearalanone in ESHA systems (Figure S7 in the Supporting Information and Table 2), suggesting similar mechanisms of transformation across the compound class. Dark controls with all species were stable over relevant time scales, suggesting no other loss processes occurred. Rather, our results are most consistent with a reaction between zeranol and reactive species generated upon irradiation of DOM [e.g., reactive oxygen species (ROS) or triplet DOM (^{3}DOM*)].

Comparison of measured $t_{1/2}$ values for zeranol to the steady-state ROS concentrations in irradiated HA and FA solutions at pH 7.0 provided an initial assessment of possible photooxidant(s) responsible for attenuation. This comparison is shown in Table S1 in the Supporting Information for steady-state concentrations of hydroxyl radical ($[^\bullet OH]_{ss}$) and singlet oxygen ($[^1O_2]_{ss}$) in DOM solutions, concentrations that were measured in the absence of zeranol. Both $^\bullet OH$ and $^1O_2$ were quantifiable in all solutions; whereas $[^\bullet OH]_{ss}$ values were roughly constant in all systems, Table S1 in the Supporting Information reveals that zeranol half-lives loosely scale with $[^1O_2]_{ss}$ values. Furthermore, as detailed in the Supporting Information, established routes for $^\bullet OH$ and $^1O_2$ formation (i.e., the Fenton reaction and $^1O_2$ sensitizers such as Rose Bengal or Erythrosin B, respectively) revealed that both oxidants are indeed reactive toward zeranol. In the Supporting Information (Figure S8), we also discuss results from competition kinetic experiments attempting to quantify second-order rate coefficients for the reaction of each ROS with zeranol.

Closer examination suggests that $^1O_2$ is most likely not responsible for zeranol loss in our HA and FA solutions at pH 7.0. Experiments conducted in the presence of excess azide (10 mM), commonly used as a quencher for $^1O_2$,[37,38] revealed no inhibition of zeranol decay relative to azide-free systems (Figure 2b). Similarly, experiments conducted in pure D_2O (Figure 2b), in which the lifetime of $^1O_2$ is greater than in H_2O thus promoting its reactivity,[39] did not exhibit enhanced rates of zeranol transformation.

Additional experiments with selective quenchers provided greater insight into the species responsible for zeranol

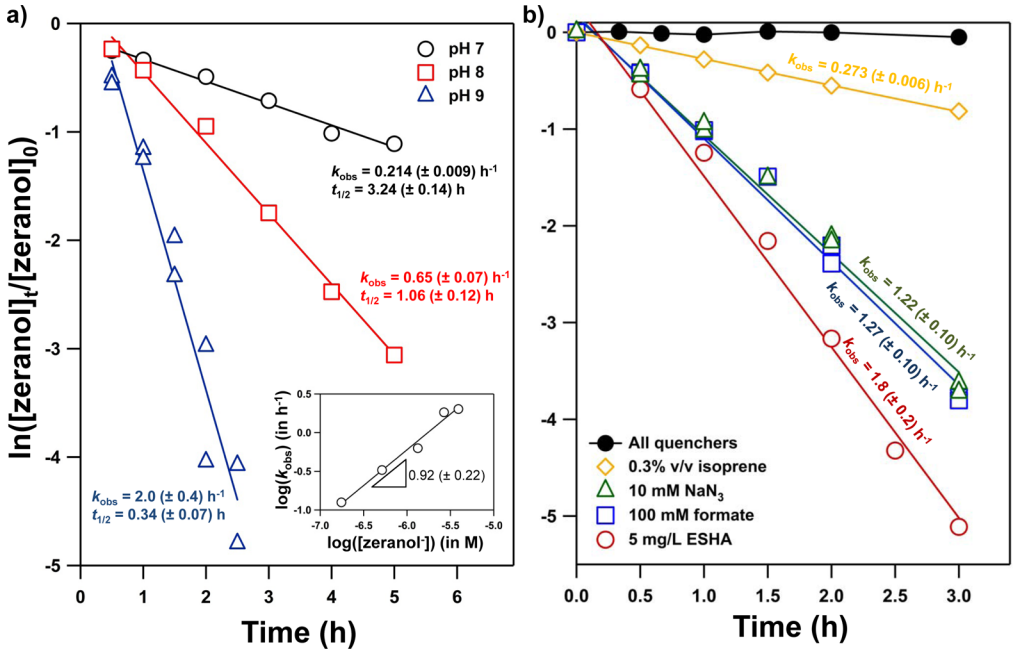

Figure 3. (a) Plots of the natural log of normalized zeranol concentration as a function of time in irradiated solutions of 5 mg/L of ESHA at pH 7, 8, and 9. Values of k_{obs} (with 95% confidence intervals) obtained from linear regression analyses are provided. The inset shows a log−log plot of k_{obs} values as a function of the concentration of the monodeprotonated form of zeranol ([zeranol$^-$]; pK_{a1} 8.44), with a slope equivalent to unity. (b) Results of quencher experiments conducted at pH 8.5 in solutions of 5 mg/L of ESHA. Values of k_{obs} (with 95% confidence intervals) obtained from linear regression analyses are provided. Given the modest decrease observed with formate and sodium azide, results from duplicate experiments are presented to illustrate reproducibility. In all instances, the initial concentration of zeranol was ∼5 μM. The pH was maintained at pH 7 and 7.5 using 5 mM phosphate buffer, while solutions at pH 8−9 were maintained with an 5 mM borate buffer.

attenuation at neutral pH. Excess formate (50−100 mM) or similar radical scavenger (e.g., isopropanol) slowed zeranol decay by roughly 50% (Figure 2c). No further inhibition was observed if higher concentrations of radical scavenger were used, suggesting that $^{\bullet}$OH contributes to some but not all of the zeranol transformation observed. Additionally, catalase, which breaks down H_2O_2, inhibited zeranol decay by a similar magnitude to that of radical scavengers (Figure S9 in the Supporting Information). Formation of H_2O_2 was quantifiable in irradiated DOM systems (Figure S10 in the Supporting Information), but it was unreactive toward zeranol in dark control systems (Figure S11 in the Supporting Information). Thus, the role of H_2O_2 in zeranol decay is likely linked to its photolysis, which generates $^{\bullet}$OH.[40] Such a scenario is supported by experiments revealing comparable zeranol decay in irradiated systems free of DOM but containing 5 μM H_2O_2 (Figure S11 in the Supporting Information), a concentration representative of that measured in our irradiated DOM suspensions. Also consistent with H_2O_2 photolysis as a major route to $^{\bullet}$OH formation, addition of superoxide dismutase, which converts superoxide radical anion ($O_2^{\bullet-}$) into H_2O_2, enhanced the rate of zeranol decay (Figure S9 in the Supporting Information). We attribute this enhancement to the subsequent photolysis of H_2O_2 produced via superoxide dismutase.

Evidence suggests that the remainder of zeranol transformation occurs via reaction with triplet, or excited state, DOM (^{3}DOM*). Zeranol decay persisted in deoxygenated systems, in which ROS should not be generated at appreciable levels, which is consistent with direct reaction with ^{3}DOM* (Figure S12 in the Supporting Information). Furthermore, the presence of 0.1% v/v isoprene, commonly utilized as a triplet quencher,[41,42] inhibited zeranol decay by ∼50% (Figure 2d), thereby accounting for the remainder of the loss we assume is not attributable to $^{\bullet}$OH (i.e., the amount of zeranol transformation observed in the presence of excess formate or isopropanol). Zeranol is moderately hydrophobic (reported logK_{ow} of 3.88),[43] and thus a small fraction would likely be associated with HA and FA in solution, which in turn would promote its direct reaction with ^{3}DOM*. A role for ^{3}DOM* in the photooxidation of zeranol is perhaps not surprising, as Canonica and co-workers[44,45] have previously established that excited triplet states generated during DOM irradiation are important photooxidants for substituted phenols, which represents reasonable structural analogues for zeranol family compounds. Finally, we note that irradiated suspensions of ESHA containing both a radical (formate) and triplet (isoprene) quencher completely shut down zeranol decay over the time scales typically observed (Figure 2d), further supporting $^{\bullet}$OH and ^{3}DOM* as dominant reactive species in our systems at pH 7.

Although zeranol decay in the ESHA system was investigated most extensively, we believe $^{\bullet}$OH and ^{3}DOM* are also dominant species at play in other HA and FA systems at neutral pH. Similar experiments with quenchers and probes with Leonardite HA (Figure S13 in the Supporting Information) were also consistent with a role for these reactive species. Further, $^{\bullet}$OH and ^{3}DOM* appear to be the key players responsible for the decay of zeranol metabolites at pH 7.0. Results from experiments with zearalanone in irradiated ESHA systems at pH 7.0 containing formate and isoprene (Figure S14 in the Supporting Information) mirror the behavior observed for zeranol.

Indirect Photolysis of Zeranol in Slightly Alkaline Solutions. The −OH groups on zeranol have reported pK_a values of 8.44 and 11.42,[26] and thus its reactivity toward

dx.doi.org/10.1021/es303091c | Environ. Sci. Technol. XXXX, XXX, XXX−XXX

photogenerated ROS is likely to increase as these groups deprotonate. Indeed, while zeranol remained photostable in the absence of ESHA with increasing pH, its rate of transformation increased by more than 1 order of magnitude in the presence of ESHA (5 mg/L) as pH increased from 7.0 to 9.0 (Figure 3a). On the basis of additional studies with phenol and furfuryl alcohol, the concentration of photogenerated $^{\bullet}OH$ and $^1O_2$, respectively, did not change significantly over this pH range. Thus, this increase in reactivity is most consistent with deprotonated forms of zeranol, which become more concentrated at higher pH values, being the primary reactivity entities toward photogenerated oxidants. The inset in Figure 3a shows a log−log plot of the k_{obs} values for zeranol decay in irradiated ESHA suspensions measured between pH 7.0 to 9.0 as a function of the corresponding concentration of the monodeprotonated form of zeranol ([zeranol$^-$]; assuming a pK_{a1} of 8.44). The slope of this log−log plot is equivalent to unity, suggesting a first-order dependence of the rate of photoreaction on the concentration of the monodeprotonated species.

Although $^1O_2$ does not appear to contribute to zeranol decay in our model DOM systems at pH 7.0, evidence suggests it may play a role in slightly alkaline pH waters. Additional experiments with selective quenchers at pH 8.5 reveal that ^{3}DOM* is still a major contributor to zeranol transformation in irradiated ESHA suspensions (Figure 3b) based on the inhibition observed in the presence of excess isoprene (0.3% v/v). Excess formate (a radical quencher) yielded a small, but reproducible, decrease in zeranol transformation consistent with a continued role for $^{\bullet}OH$ at pH 8.5. Unlike at pH 7.0, the use of 10 mM sodium azide, a $^1O_2$ quencher, also resulted in a modest yet reproducible amount of inhibition. Most importantly, complete suppression of zeranol decay at pH 8.5 was only observed in systems with all three quenchers present, consistent with ^{3}DOM*, $^{\bullet}OH$, and $^1O_2$ all contributing to zeranol decay to some extent. Thus, while the contribution of $^1O_2$ to zeranol decay appears negligible at neutral pH, it appears to become more significant with an increasing pH value. We assume this increase is because of its greater reactivity toward anionic zeranol species.

Photolysis of SGPMs in Neutral pH Natural Waters. Finally, additional experiments with natural water samples indicate that the phototransformation mechanism observed in model aquatic systems also occur in more complicated waters representative of agriculturally impacted ecosystems. Rates of direct photolysis for 17β-trenbolone were essentially equivalent in circumneutral pH water (pH 6.8−7.0) collected from a runoff-impacted, high DOC creek (50 mg/L) and a low DOC agricultural return water (6 mg/L). Moreover, these rates compared favorably to that measured in model systems of phosphate buffer (Figure S15a,b in the Supporting Information). Addition of ROS quenchers including formate and isoprene had no effect on 17β-trenbolone transformation rate, nor was the decay rate influenced when experiments were conducted in a 50:50 mixture of natural water sample and D_2O. Thus, despite the presence of relatively high DOC concentrations, indirect routes for 17β-trenbolone photolysis are sufficiently slow relative to direct photolysis so as not to impact its persistence. We believe this to be generally true for all compounds in the TBA and MGA families.

Zeranol loss was observed upon irradiation of both natural water samples, with the greatest rate of transformation occurring in the high DOC creek water rather than the agricultural return water (Figure S15c,d in the Supporting Information). Rates of zeranol decay were within the range reported for 5 mg/L solutions of model humic and fulvic acids, and use of formate and isoprene as $^{\bullet}OH$ and triplet DOM quenchers, respectively, inhibited zeranol transformation. Collectively, as was observed in model systems, results are consistent with indirect photolysis influencing the fate of zeranol in sunlit surface waters, with a prominent role for $^{\bullet}OH$ and ^{3}DOM* at neutral pH.

Preliminary Assessment of Direct Photolysis Products. Because of the relatively rapid rate of TBA and MGA family direct photolysis, information on the photoproducts generated via this process will be essential to assessing fully their impact on ecosystem health. We present an introduction to these photoproducts here, while an extensive treatment of the identity, fate and ecotoxicological impacts of these direct photoproducts is the subject of a future study.

Within a compound class, no interspecies conversions were observed (e.g., based on comparison of known LC retention times, photolysis of 17β-trenbolone did not yield 17α-trenbolone or trendione, nor did photolysis of MGA yield melengestrol). Instead, both families of compounds photolyzed to yield mixtures of new species that are usually more polar (i.e., products elute earlier on a reverse phase LC column). Further, they exhibit primary absorption maxima at lower wavelengths outside the solar spectrum (Figure S16 in the Supporting Information). This is consistent with some degree of disruption to the conjugated π-bond systems characteristic to these species during photolysis. Analysis with LC/MS/MS suggests that direct photolysis yields rather modest structural transformations for these compounds, with most reaction products maintaining the steroidal ring and forming via simple hydroxyl addition (e.g., masses detected for 17β-trenbolone were m/z 289, 305, and 321, representing mono-, di-, and trihydroxy derivatives). We also cannot completely rule out the potential for photoisomerization at other stereochemical centers within TBA and MGA metabolites (e.g., methyl inversion at the C13 in TBA metabolites), as has been observed during the direct photolysis of estrone.[46]

On the basis of these observations, photoproducts appear to be more, if not entirely, resistant to direct photolysis via sunlight and are likely to persist in sunlit surface waters longer than the species from which they are derived. Given the slight structure modifications induced by direct photolysis, these more photoresistant products are also likely to retain some biochemical activity similar to their parents, the magnitude of which will be addressed in a future investigation.

Environmental Implications. This work provides some of the first evidence characterizing the persistence of synthetic hormone growth promoters in sunlit surface waters impacted by agricultural runoff. The trenbolone acetate and melengestrol acetate families, which share conjugated π-bond systems within their steroidal ring structure, are prone to direct photolysis and are likely to exhibit the least amount of persistence. They exhibit relatively short half-lives (1 h or less), and their decay rates are largely invariant across a broad spectrum of aquatic conditions, implying that direct photolysis will be their dominant transformation mechanism in most sunlit surface waters. Indeed, relative to reports of their biotransformation in aerobic soil microcosms,[47] time scales for the photolysis of TBA metabolites are considerably faster, although these transformation pathways are unlikely to compete with one another given their tendency to be localized in different environmental media. The near-constant rates of photolysis

measured over the range of aquatic conditions considered may be advantageous; fate models should be able to better account for the contribution of photolysis to these species' environmental persistence.

Nonsteroidal zeranol and its metabolites, which have little to no chromophoric activity within the solar spectrum, only transform via indirect photolysis. Therefore, their fate may be more difficult to predict because it will be highly dependent on the composition of the receiving water, with variables such as DOM concentration, type, and pH exerting an influence. The presence of sensitizers or other species that generate $^{\bullet}OH$ or $^{1}O_2$ (at higher pH) will shorten the lifetime of the zeranol family, whereas known scavengers (e.g., carbonate for $^{\bullet}OH$) would inhibit their indirect phototransformation. For example, we have conducted preliminary work with nitrate, another common agricultural byproduct that photolyzes to yield $^{\bullet}OH$[48] (Figure S17 in the Supporting Information), confirming its ability to facilitate zeranol transformation. A role for triplet state DOM in zeranol transformation is also noteworthy because zeranol and its metabolites are moderately hydrophobic and therefore a small fraction of it will be associated organic colloids in surface waters. While bound to such organic colloids they may be more recalcitrant to biotransformation but will be highly prone to DOM-sensitized photolysis. We note that in addition to improving our understanding of zeranol and its metabolites in the environment, these insights should also prove useful in predicting the behavior of mycotoxins related to zearalenone, many of which are structurally analogous to zeranol.

Transformation has often been equated with removal and mitigation of ecological risk. However, initial evidence about the products from the direct photolysis of the TBA and MGA families suggests minor structural modifications and is most consistent with conservation of the steroid ring structure after reaction. Given the short time scales associated with phototransformation and the lower photoactivity of these product mixtures, this work emphasizes the need for detailed isolation, identification, and fate assessment for the phototransformation products of SGPMs. Such transformation products may have profound impact on ecosystem health, particularly given the anabolic potency of the parent compounds from which they are derived. In a future work, we intend to systematically explore the identity and structure of products from the photolysis of the TBA and MGA families and consider the potential ecotoxicological risks associated with their formation.

■ ASSOCIATED CONTENT

Supporting Information

Additional methods including details of quantum yield measurements, quencher and probe studies, as well as additional results from photochemical batch experiments. This material is available free of charge via the Internet at http://pubs.acs.org.

■ AUTHOR INFORMATION

Corresponding Author

*E-mail: david-cwiertny@uiowa.edu; phone: 319-335-1401; fax: 319-335-5660.

Notes

The authors declare no competing financial interest.

■ ACKNOWLEDGMENTS

This work is supported through a USDA Agriculture Food Research Initiative (AFRI) Water and Watersheds Grant No. 2010-65102-20425. The authors would like to acknowledge Prof. Doug Latch for insightful discussions on interpretation of results from photolysis experiments. The authors would also like to thank the three anonymous reviewers whose feedback greatly improved the quality of this work.

■ REFERENCES

(1) Bloss, R. E.; Northam, J. I.; Smith, L. W.; Zimbelman, R. G. Effects of oral melengestrol acetate on the performance of feedlot cattle. *J. Anim. Sci.* **1966**, *25*, 1048−1053.

(2) Lee, L. S.; Carmosini, N.; Sassman, S. A.; Dion, H. M.; Sepúlveda, M. S. Agricultural contributions of antimicrobials and hormones on soil and water quality. *Adv. Agron.* **2007**, *93*, 1−68.

(3) Lefebvre, B.; Malouin, F.; Roy, G.; Giguére, K.; Diarra, M. S. Growth performance and shedding of some pathogenic bacteria in feedlot cattle treated with different growth-promoting agents. *J. Food Protect.* **2006**, *69*, 1256−1264.

(4) Sinnett-Smith, P. A.; Dumelow, N. W.; Buttery, P. J. Effects of trenbolone acetate and zeranol on protein metabolism in male castrate and female lambs. *Br. J. Nutr.* **1983**, *50*, 225−34.

(5) Balter, M. Scientific cross-claims fly in continuing beef war. *Science* **1999**, *284*, 1453−1455.

(6) California Environmental Contaminant Biomonitoring Program (CECBP) Scientific Guidance Panel (SGP). *Synthetic Hormones in Animal Husbandry*, 2008. Available at oehha.ca.gov/multimedia/biomon/pdf/120408synhormonesdoc.pdf.

(7) Neumann, F. Pharmacological and Endocrinological Studies on Anabolic Agents. In *Anabolic Agents in Animal Production*; Lu, F. C., Rendel, J., Eds.; Thieme Publishers: Stuttgart, Germany, 1976; pp 253−264.

(8) Lauderdale, J. W. Use of Melengestrol Acetate in Animal Production. In *Proceedings of the Symposium on Anabolics in Animal Production: Public Health Aspects, Analytical Methods, and Regulation*; Meissonnier, E., Mitchell-Vigneron, J., Eds.; Office International des Epizooties: Paris, France, 1983; pp 193−212.

(9) Pottier, J.; Cousty, C.; Heitzman, R. J.; Reynolds, I. P. Differences in the biotransformation of a 17β-hydroxylated steroid, trenbolone acetate, in rat and cow. *Xenobiotica* **1981**, *11*, 489−500.

(10) Krzeminski, L. F.; Cox, B. L.; Gosline, R. E. Fate of radioactive melengestrol acetate in the bovine. *J. Agric. Food Chem.* **1981**, *29*, 387−391.

(11) Upjohn Company. *Environmental Assessment: Melengestrol Acetate (MGA) for Suppression of Estrus for Heifers Intended for Breeding*; 1996. Available at http://www.fda.gov/cvm/FOI/034-254EA.pdf

(12) Kleinova, M.; Zöllner, P.; Kahlbacher, H.; Hochsteiner, W.; Lindner, W. Metabolic profiles of the mycotoxin zearalenone and of the growth promoter zeranol in urine, liver, and muscle of heifers. *J. Agric. Food Chem.* **2002**, *50*, 4769−4776.

(13) Kolok, A. S.; Sellin, M. K. The environmental impact of growth-promoting compounds employed by the United States beef cattle industry: history, current knowledge, and future directions. *Rev. Environ. Contam. Toxicol.* **2008**, *195*, 1−30.

(14) Bartelt-Hunt, S. L.; Snow, D. D.; Kranz, W. L.; Mader, T. L.; Shapiro, C. A.; van Donk, S. J.; Shelton, D. P.; Tarkalson, D. D.; Zhang, T. C. Effect of growth promotants on the occurrence of endogenous and synthetic steroid hormones on feedlot soils and in runoff from beef cattle feeding operations. *Environ. Sci. Technol.* **2012**, *46*, 1352−1360.

(15) Durhan, E. J.; Lambright, C. S.; Makynen, E. A.; Lazorchak, J.; Hartig, P. C.; Wilson, V. S.; Gray, L. E.; Ankley, G. T. Identification of metabolites of trenbolone acetate in androgenic runoff from a beef feedlot. *Environ. Health Perspect.* **2006**, *1*, 65−68.

(16) Gall, H. E.; Sassman, S. A.; Lee, L. S.; Jafvert, C. T. Hormone discharges from a midwest tile-drained agroecosystem receiving animal wastes. *Environ. Sci. Technol.* **2011**, *45*, 8755−8764.
(17) Kolok, A. S.; Snow, D. D.; Kohno, S.; Sellin, M. K.; Guillette, L. J., Jr Occurrence and biological effect of exogenous steroids in the Elkhorn River, Nebraska, USA. *Sci. Total Environ.* **2007**, *388*, 104−115.
(18) Laganà, A.; Bacaloni, A.; De Leva, I.; Faberi, A.; Fago, G.; Marino, A. Analytical methodologies for determining the occurrence of endocrine disrupting chemicals in sewage treatment plants and natural waters. *Anal. Chim. Acta* **2004**, *501*, 79−88.
(19) Schiffer, B.; Daxenberger, A.; Meyer, K.; Meyer, H. H. The fate of trenbolone acetate and melengestrol acetate after application as growth promoters in cattle: environmental studies. *Environ. Health Perspect.* **2001**, *109*, 1145−51.
(20) Ankley, G. T.; Jensen, K. M.; Makynen, E. A.; Kahl, M. D.; Korte, J. J.; Hornung, M. W.; Henry, T. R.; Denny, J. S.; Leino, R. L.; Wilson, V. S.; Cardon, M. C.; Hartig, P. C.; Gray, L. E. Effects of the androgenic growth promoter 17-beta-trenbolone on fecundity and reproductive endocrinology of the fathead minnow. *Environ. Toxicol. Chem.* **2003**, *22*, 1350−60.
(21) Bauer, E. R.; Daxenberger, A.; Petri, T.; Sauerwein, H.; Meyer, H. H. Characterisation of the affinity of different anabolics and synthetic hormones to the human androgen receptor, human sex hormone binding globulin and to the bovine progestin receptor. *APMIS* **2000**, *108*, 838−46.
(22) Jensen, K. M.; Makynen, E. A.; Kahl, M. D.; Ankley, G. T. Effects of the feedlot contaminant 17α-trenbolone on reproductive endocrinology of the fathead minnow. *Environ. Sci. Technol.* **2006**, *40*, 3112−7.
(23) Lauderdale, J. W.; Goyings, L. S.; Krzeminski, L. F.; Zimbelman, R. G. Studies of a progestogen (MGA) as related to residues and human consumption. *J. Photochem. Photobiol. A* **1977**, *3*, 5−33.
(24) van der Merwe, P. J.; Pieterse, J. W. Stability of zeranol, nandrolone and trenbolone in bovine urine. *Analyst* **1994**, *119*, 2651−3.
(25) Gryglik, D.; Olak, M.; Miller, J. S. Photodegradation kinetics of androgenic steroids boldenone and trenbolone in aqueous solutions. *J. Photochem. Photobiol. A* **2010**, *212*, 14−19.
(26) Mallinckrodt Veterinary, Inc. Environmental Assessment for Zeranol; 1994. Available at http://www.fda.gov/cvm/FOI/038-233EA.pdf.
(27) Syntex Animal Health. *Synovex Plus (trenbolone acetate and estradiol benzoate) Implant Environmental Assessment*; 1995. Available at www.fda.gov/cvm/FOI/141-043EA.pdf
(28) Kuhn, H. J.; Braslavsky, S. E.; Schmidt, R. Chemical Actinometry (IUPAC technical report). *Pure Appl. Chem.* **2004**, *76*, 2105−2146.
(29) Leifer, A. *The Kinetics of Environmental Aquatic Photochemistry: Theory and Practice*; American Chemical Society: Washington, DC, 1988.
(30) Dulin, D.; Mill, T. Development and evaluation of sunlight actinometers. *Environ. Sci. Technol.* **1982**, *16*, 815−820.
(31) Khan, S. J.; Roser, D. J.; Davies, C. M.; Peters, G. M.; Stuetz, R. M.; Tucker, R.; Ashbolt, N. J. Chemical contaminants in feedlot wastes: Concentrations, effects and attenuation. *Environ. Int.* **2008**, *34*, 839−859.
(32) Schiffer, B.; Totsche, K. U.; Jann, S.; Kögel-Knabner, I.; Meyer, K.; Meyer, H. H. D. Mobility of the growth promoters trenbolone and melengestrol acetate in agricultural soil: column studies. *Sci. Total Environ.* **2004**, *326*, 225−237.
(33) Kim, H. L.; Ray, A. C.; Stipanovic, R. D. Rapid separation and identification of urinary metabolites of zeranol by HPLC-UV spectrophotometry. *J. Agric. Food Chem.* **1986**, *34*, 312−315.
(34) Visconti, A.; Pascale, M. Determination of zearalenone in corn by means of immunoaffinity clean-up and high-performance liquid chromatography with fluorescence detection. *J. Chromatogr., A* **1998**, *815*, 133−140.
(35) Vulliet, E.; Falletta, M.; Marote, P.; Lomberget, T.; Païssé, J.-O.; Grenier-Loustalot, M.-F. Light induced degradation of testosterone in waters. *Sci. Total Environ.* **2010**, *408*, 3554−3559.
(36) Lin, A. Y.-C.; Reinhard, M. Photodegradation of common environmental pharmaceuticals and estrogens in river water. *Environ. Toxicol. Chem.* **2005**, *24*, 1303−1309.
(37) Werner, J. J.; McNeill, K.; Arnold, W. A. Environmental photodegradation of mefenamic acid. *Chemosphere* **2005**, *58*, 1339−1346.
(38) Zhang, T.; Hsu-Kim, H. Photolytic degradation of methylmercury enhanced by binding to natural organic ligands. *Nat. Geosci.* **2010**, *3*, 473−476.
(39) Parker, J. G.; Stanbro, W. D. Optical determination of the rates of formation and decay of $O_2(^1\Delta_g)$ in H_2O, D_2O and other solvents. *J. Photochem.* **1984**, 545−547.
(40) Kochany, J.; Bolton, J. R. Mechanism of photodegradation of aqueous organic pollutants. 2. Measurements of the primary rate constants for reaction of hydroxyl radicals with benzene and some halobenzenes using an EPR spin-trapping method following the photolysis of hydrogen peroxide. *Environ. Sci. Technol.* **1992**, *26*, 262−265.
(41) Zepp, R. G.; Schlotzhauer, P. F.; Sink, R. M. Photosensitized transformations involving electronic energy transfer in natural waters: role of humic substances. *Environ. Sci. Technol.* **1985**, *19*, 74−81.
(42) Boreen, A. L.; Arnold, W. A.; McNeill, K. Triplet-Sensitized Photodegradation of sulfa drugs containing six-membered heterocyclic groups: Identification of an SO_2 extrusion photoproduct. *Environ. Sci. Technol.* **2005**, *39*, 3630−3638.
(43) Card, M. L.; Chin, Y.-P.; Lee, L. S.; Khan, B. Prediction and Experimental Evaluation of Soil Sorption by Natural Hormones and Hormone Mimics. *J. Agric. Food Chem.* **2011**, *60*, 1480−1487.
(44) Canonica, S.; Jans, U.; Stemmler, K.; Hoigné, J. Transformation kinetics of phenols in water: photosensitization by dissolved natural organic material and aromatic ketones. *Environ. Sci. Technol.* **1995**, *29*, 1822−1831.
(45) Canonica, S.; Hellrung, B.; Wirz, J. Oxidation of phenols by triplet aromatic ketones in aqueous solution. *J. Phys. Chem. A* **2000**, *104*, 1226−1232.
(46) Trudeau, V. L.; Heyne, B.; Blais, J. M.; Temussi, F.; Atkinson, S. K.; Pakdel, F.; Popesku, J. T.; Marlatt, V. L.; Scaiano, J. C.; Previtera, L.; Lean, D. R. S. Lumiestrone is photochemically derived from estrone and may be released to the environment without detection. *Front. Endocrinol.* **2011**, *2*, 1−13.
(47) Khan, B.; Lee, L. S.; Sassman, S. A. Degradation of synthetic androgens 17α- and 17β-trenbolone and trendione in agricultural soils. *Environ. Sci. Technol.* **2008**, *42*, 3570−3574.
(48) Zepp, R. G.; Hoigne, J.; Bader, H. Nitrate-induced photooxidation of trace organic chemicals in water. *Environ. Sci. Technol.* **1987**, *21*, 443−450.